J|A|C|S ARTICLES

Published on Web 02/16/2010

Synthesis and Structural Determination of Multidentate 2,3-Dithiol-Stabilized Au Clusters

Zhenghua Tang, Bin Xu, Baohua Wu, Markus W. Germann, and Gangli Wang*

Department of Chemistry, Georgia State University, Atlanta, Georgia 30302

Received September 8, 2009; E-mail: glwang@gsu.edu

Abstract: Interface bond structure, in addition to the well-known size and shape quantum confinement effects, is another factor that affects the properties of nanomaterials that is less known and studied. Inspired by the thiol-bridging "staple" motif (RS−Au−SR, Jadzinsky; et al. *Science* **2007**, *318*, 430.) discovered from monothiol-stabilized gold nanoclusters, dithiol ligand 2,3-dimercaptopropanesulfonic (DMPS) acid has been employed to synthesize dithiol-protected Au clusters (DTCs). The structure and property of the Au DTCs are studied to probe two effects: the entropy gain of dithiol over monothiol ligand protection and the constraint to the formation of the thiol bridging surface bonding. The hydrodynamic sizes of Au DTCs were estimated by diffusion nuclear magnetic resonance (NMR). The size distribution, Au core plus ligands on solid support, was confirmed by atomic force microscope (AFM) imaging. Size-dependent optical properties were observed. Au_4 clusters at high purity, characterized by mass spectrometry and organic−metal ratio confirmed by thermogravimetric analysis (TGA), display a characteristic absorbance band at 282 nm. The proton chemical environments as well as Au−S bond information of the Au_4 cluster were fully elucidated by $^{13}C-^{1}H$ heteronuclear single-quantum coherence (HSQC) in conjunction with other two-dimensional (2D) NMR techniques. The Au−S bonding was further studied in thiol stretching by infrared and Au(4f) and S(2p) electrons by X-ray photoelectron spectroscopy (XPS). One possible structure of the Au_4 cluster has been proposed that needs further theoretical studies or single-crystal confirmation.

Introduction

Au nanoparticles and small clusters have attracted continuous research interest over decades due to their rich optical features, electrochemical properties, and surface functionalities, which render them extensive potentials in nanoelectronics, biomedicine, and catalysis applications.[1−3] It is well-known that size and shape affect nanomaterials properties due to quantum confinement effects. In the context of sub-2-nm Au clusters, recent breakthroughs have revealed a novel thiol bridging surface Au−S bonding motif, experimentally discovered by X-ray single crystallography[4−6] and theoretically predicted by density function theory calculations.[7−9] The immediate questions to address next would be: what properties are affected by the novel surface bond structure; to what extent are the properties affected; and ultimately can the bond formation be manipulated to create new clusters with novel properties? The approach of this paper is illustrated in Figure 1. Inspired by the thiol-bridging structure illustrated on the left panel, a dithiol molecule with two adjacent thiol groups, 2,3-dimercaptopropanesulfonate (DMPS) shown on the right, has been employed to synthesize Au dithiol clusters (DTCs). While entropy gain is expected if both thiol groups bind to Au (one dithiol molecule taking the places of two monothiol molecules), the constraint by linking two thiol groups on the same molecule would have an impact on the thiol-bridging bonding motif, which could result in novel properties compared to the well-established monothiol Au MPCs.

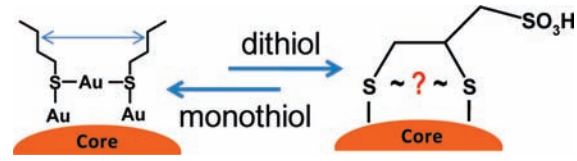

Figure 1. Structural illustration of two monothiol molecules versus one dithiol molecule on Au core surface. (Left) Thiol-bridging motif discovered on monothiol MPC.[4] (Right) DMPS dithiol on core surface.

Au clusters with core size a few nanometers or less are of extensive interests not only in fundamental studies but also in practical applications. In the biological and medical regime, to be efficiently excreted by body clearance to avoid prolonged stay in various tissues, a criteria has recently been reported of less than 5.5 nm hydrodynamic diameter and nonadsorptive coating for nanomaterials.[10] In catalysis, recent experiments

(1) Murray, R. W. *Chem. Rev.* **2008**, *108*, 2688–2720.
(2) Daniel, M.-C.; Astruc, D. *Chem. Rev.* **2004**, *104*, 293–346.
(3) Han, G.; Ghosh, P.; Rotello, V. M. *Nanomed* **2007**, *2* (1), 113–123.
(4) Jadzinsky, P. D.; Calero, G.; Ackerson, C. J.; Bushnell, D. A.; Kornberg, R. D. *Science* **2007**, *318*, 430–432.
(5) Heaven, M. W.; Dass, A.; White, P. S.; Holt, K. M.; Murray, R. W. *J. Am. Chem. Soc.* **2008**, *130*, 3754–3755.
(6) Zhu, M.; Aikens, C. M.; Hollander, F. J.; Schatz, G. C.; Jin, R. *J. Am. Chem. Soc.* **2008**, *130*, 5883–5885.
(7) Akola, J.; Walter, M.; Whetten, R. L.; Hakkinen, H.; Gronbeck, H. *J. Am. Chem. Soc.* **2008**, *130*, 3756–3757.
(8) Jiang, D.-e.; Tiago, M. L.; Luo, W.; Dai, S. *J. Am. Chem. Soc.* **2008**, *130*, 2777–2779.
(9) Walter, M.; Akola, J.; Lopez-Acevedo, O.; Jadzinsky, P. D.; Calero, G.; Ackerson, C. J.; Whetten, R. L.; Gronbeck, H.; Hakkinen, H. *Proc. Natl. Acad. Sci. U.S.A.* **2008**, *105*, 9157–9162.
(10) Soo Choi, H.; Liu, W.; Misra, P.; Tanaka, E.; Zimmer, J. P.; Itty Ipe, B.; Bawendi, M. G.; Frangioni, J. V. *Nat. Biotechnol.* **2007**, *25*, 1165–1170.

indicate that sub-2 nanometer gold clusters might be the most active species for CO oxidation.[11] To tailor the size of Au nanoclusters, extensive efforts have been devoted to control the thermodynamics and kinetics of the core agglomeration and surface passivation. The factors such as solvent polarity, reaction temperature, and mixing conditions in the synthesis have been systematically studied.[1,12−14] In the context of ligand molecules, most successes to synthesize small stable clusters have been achieved by using bulky and polymeric ligands and by adopting a high ligand-to-metal ratio in the synthesis.[15−19]

Multidentate ligands have been widely used in inorganic and analytical chemistry in the context of chelates or metal−ligand complexes. Oligonuclear Au complexes with thiol, ylide, phosphine, or other complexing agents have been developed as therapeutic agents and as fluorophores for decades and continue to be extensively explored.[20−24] While polydisperse Au(I)−thiolate complexes are known to be the intermediates to the formation of Au MPCs or nanoparticles before the reduction by $NaBH_4$, recent experimental and theoretical results suggest that $(AuSR)_4$ complexes are key units in the formation of monothiol Au MPCs and ligand exchange reactions.[25−27]

Multidentate approach has recently been employed to enhance surface layer stability of nanomaterials with the consideration of the entropy effects. Semiconductor quantum dots with tuned and miniaturized hydrodynamic sizes have been synthesized.[28,29] Aggregation of metal nanoparticles of larger sizes was effectively inhibited by designed multithiols by Lee and co-workers.[30−32] Dihydrolipoic acid (1,3-dithiol) has been used to directly synthesize Au nanoparticles.[33,34] Without the reduction by $NaBH_4$, various Au(I) complexes have been synthesized by employing meso-2,3 dithiol dimercaptosuccinic acid by the Tsukuda group.[35] Multithiol anchored oligonucleotide−Au nanoparticles have also been reported with improved stabilities.[36,37] With the novel S−Au−S bonding motif discovered, we believe that employing the multidentate approach would significantly enhance our ability to control the nanomaterials formation process, thereby achieving better size control. More importantly, it could result in novel bonding structures due to the constraint imposed by the linker between the multidentate sites within the individual ligand. In this paper, Au DTCs stabilized by DMPS ligands have been synthesized and characterized. Size transition from small Au_4 complexes up to ∼3 nm Au DTCs is achieved. The structure and properties of the Au DTCs tailored by controlling the dithiol:Au ratio in the synthesis are reported.

Experimental Section

Chemicals. Tetrachloroauric acid ($HAuCl_4 \cdot 3H_2O$, >99.99% metals basis, Aldrich), sodium 2,3-dimercaptopropanesulfonate monohydrate ($C_3H_7O_3S_3Na \cdot H_2O$, ∼95%, Aldrich), sodium borohydride ($NaBH_4$, 99%, Aldrich) were used as received. Water (18.2 MΩ·cm) was purified by the Barnstead Nanopure system. Other chemicals were used without further purification.

Measurements. UV−visible absorbance spectra were recorded with a Shimadzu UV-1700 spectrophotometer. Mass spectrometry spectra were acquired on ABI 4800 MALDI TOF-TOF analyzer. Widely used for small protein analysis, α-cyano-4-hydroxycinnamic acid (CHCA) was used as matrix. XPS analysis was conducted with a SSX-100 X-ray photoelectron spectrometer (Surface Science Laboratories Inc., Georgia Institute of Technology Nanotechnology Research Center) using an Al Kα X-ray source (1486.6 eV) with the analysis chamber pressure lower than 1×10^{-8} Torr. Atomic force microscope (AFM) images were collected with a MultiMode instrument (Veeco) under tapping mode. The tips used in all measurements were LTESP (Veeco, USA) with a radius of ∼10 nm. A Perkin-Elmer Spectrum 100 FT-IR spectrometer was employed in the infrared studies. Thermogravimetric analysis (TGA) was performed with a Seiko RTG 220 robotic TGA system, on 3−5 mg purified materials, and recorded from 25 to 1000 °C at a heating rate of ∼3 °C/min. Luminescence was tested with a Horiba Jobin-Yvon Fluorolog 311 spectrometer with T channel, through which a PMT detector in visible range and an InGaAs near IR detector (800−1500 nm) can be used. The optical spectrum of the Au DTCs is collected in aqueous solution.

For NMR analysis, the samples were dissolved in D_2O. Proton NMR (one-dimensional [1D]) spectra were acquired on a Bruker Avance 400 MHz spectrometer. Diffusion ordered spectroscopy (DOSY) measurements were performed on a 600 MHz Bruker Avance equipped with a 10A gradient amplifier using a 5 mm QXI probehead ^1H (^{31}P, ^{13}C, ^{15}N) with a shielded *Z*-gradient coil. To reduce the effects of convection during the diffusion experiment, the data was acquired at 25 °C with nitrogen with flow rate of 535 $L \cdot h^{-1}$. Furthermore, the pulse sequence consisting a double stimulated echo with bipolar gradient pulses was utilized to reduce the constant velocity effects of convection.[38] The gradient pulse duration was set to 1.5 ms with a diffusion time of 200 ms. The gradient strength was increased linearly over 16 experiments from 2 to 95% of the maximum at 53 $G \cdot cm^{-1}$ for the probe. Typically, 32 scans were accumulated to increase signal-to-noise ratio for each

(11) Herzing, A. A.; Kiely, C. J.; Carley, A. F.; Landon, P.; Hutchings, G. J. *Science* **2008**, *321*, 1331–1335.
(12) Zhu, M.; Andersen, U. N.; Jin, R. *J. Phys. Chem. A* **2009**, *113*, 4281–4284, Facile.
(13) Zhu, M.; Lanni, E.; Garg, N.; Bier, M. E.; Jin, R. *J. Am. Chem. Soc.* **2008**, *130*, 1138–1139.
(14) Tsunoyama, H.; Ichikuni, N.; Tsukuda, T. *Langmuir* **2008**, *24*, 11327–11330.
(15) Schaaff, T. G.; Whetten, R. L. *J. Phys. Chem. B* **1999**, *103*, 9394–9396.
(16) Negishi, Y.; Nobusada, K.; Tsukuda, T. *J. Am. Chem. Soc.* **2005**, *127*, 5261–5270.
(17) Tsunoyama, H.; Nickut, P.; Negishi, Y.; Al-Shamery, K.; Matsumoto, Y.; Tsukuda, T. *J. Phys. Chem. C* **2007**, *111*, 4153–4158.
(18) Shichibu, Y.; Negishi, Y.; Tsukuda, T.; Teranishi, T. *J. Am. Chem. Soc.* **2005**, *127*, 13464–13465.
(19) Duan, H.; Nie, S. *J. Am. Chem. Soc.* **2007**, *129*, 2412–2413.
(20) Shaw, C. F. *Chem. Rev.* **1999**, *99*, 2589–2600.
(21) Fackler, J. P. *Inorg. Chem.* **2002**, *41*, 6959–6972.
(22) Yam, V. W.-W.; Cheng, E. C.-C. *Chem. Soc. Rev.* **2008**, *37*, 1806–1813.
(23) Omary, M. A.; Mohamed, A. A.; Rawashdeh-Omary, M. A.; Fackler, J. P. *Coordi. Chem. Rev.* **2005**, *249*, 1372–1381.
(24) Schmid, G., Ed. *Clusters and Colloids: From Theory to Applications*; VCH: Weinheim, Germany, 1994.
(25) Gies, A. P.; Hercules, D. M.; Gerdon, A. E.; Cliffel, D. E. *J. Am. Chem. Soc.* **2007**, *129*, 1095–1104.
(26) Dass, A.; Stevenson, A.; Dubay, G. R.; Tracy, J. B.; Murray, R. W. *J. Am. Chem. Soc.* **2008**, *130*, 5940–5946.
(27) Hakkinen, H.; Walter, M.; Gronbeck, H. *J. Phys. Chem. B* **2006**, *110*, 9927–31.
(28) Smith, A. M.; Nie, S. *J. Am. Chem. Soc.* **2008**, *130*, 11278–11279.
(29) Kairdolf, B. A.; Smith, A. M.; Nie, S. *J. Am. Chem. Soc.* **2008**, *130*, 12866–12867.
(30) Srisombat, L.-o.; Park, J.-S.; Zhang, S.; Lee, T. R. *Langmuir* **2008**, *24*, 7750–7754.
(31) Zhang, S.; Leem, G.; Srisombat, L.-o.; Lee, T. R. *J. Am. Chem. Soc.* **2008**, *130*, 113–120.
(32) Krpetic, Z.; Nativo, P.; Porta, F.; Brust, M. *Bioconjugate Chem.* **2009**, *20*, 619–624.
(33) Roux, S.; Garcia, B.; Bridot, J. L.; Salome, M.; Marquette, C.; Lemelle, L.; Gillet, P.; Blum, L.; Perriat, P.; Tillement, O. *Langmuir* **2005**, *21*, 2526–2536.
(34) Abad, J. M.; Mertens, S. F. L.; Pita, M.; Fernandez, V. M.; Schiffrin, D. J. *J. Am. Chem. Soc.* **2005**, *127*, 5689–5694.
(35) Negishi, Y.; Tsukuda, T. *J. Am. Chem. Soc.* **2003**, *125*, 4046–4047.
(36) Li, Z.; Jin, R.; Mirkin, C. A.; Letsinger, R. L. *Nucleic Acids Res.* **2002**, *30*, 1558–1562.
(37) Dougan, J. A.; Karlsson, C.; Smith, W. E.; Graham, D. *Nucleic Acids Res.* **2007**, *35*, 3668–3675.
(38) Jerschow, A.; Muller, N. *J. Magn. Reson.* **1997**, *125*, 372–375.

experiment. DOSY spectra were processed using the DOSY package of XwinNMR 3.5. Two-dimensional (2D) $^{1}H-^{1}H$ correlated spectroscopy (COSY), total correlation spectroscopy (TOCSY), and $^{13}C-^{1}H$ heteronuclear single-quantum coherence (HSQC) spectra were collected on Varian Inova 500 and 600 MHz spectrometers.

Synthesis of DMPS Clusters. The DMPS clusters were synthesized and purified with a modified procedure of water-soluble monothiol Au MPC synthesis.[39,40] Based on the strategy used to synthesize smaller core sizes by using higher monothiol:Au ratios,[1] dithiol:Au ratios were varied in the synthesis at 1:2, 1:1, 2:1, 3:1, and 6:1, denoted as $n\times$ respectively. In a typical 3× (DMPS:Au) synthesis, 70.0 mg of DMPS sodium salt (0.32 mmol) and 39.4 mg of gold chloride trihydrate (0.1 mmol) were codissolved in 10 mL of Nanopure water. As Au(III) is reduced in dithiol solution,[35] referred to as intermediate,[41,42] the solution color became lighter within minutes. After 30 minutes, the absorbance spectrum stabilized but the color is still light yellow. Reductant $NaBH_4$ (38 mg, 1 mmol) in 5 mL of Nanopure water was added into the Au−dithiol mixture under vigorous stirring at 0 °C ice bath. The solution turned brown within a few minutes. Final solid of 3× and 6× are brown. The DTCs at lower thiol:Au ratio (0.5×, 1×) appear to be black. The solvent was removed by rotary evaporation at room temperature after 3-h reaction.

The crude product was easily soluble in water and purified by dialysis with cellulose ester or regenerated cellulose dialysis tube (MWCO 500 or 3500). The pH of the crude product solution was adjusted to ~1 with concentrated HCl prior to dialysis under slow stirring in a 2 L beaker filled with Nanopure water. Fresh Nanopure water was recharged every 12 h over 72-h period.[25,43] In the last step, solvent was removed under vacuum at room temperature. Effective removal of free ligands from the final materials was confirmed by 1D proton NMR spectroscopy. The final products of 0.5×, 1×, and 2× appeared to be black, while the 3× and 6× appear to be dark brown. The final clusters remained stable after repeated drying−dissolving procedures.

Results and Discussion

UV−Visible Absorbance of DMPS Clusters. UV−visible absorbance spectroscopy was used to monitor the synthesis and to characterize the products, as the extinction coefficient changes with respect to Au oxidation states and cluster size. Figure 2 shows the absorbance spectra of DTCs and the 3× intermediate (before $NaBH_4$ reduction). A characteristic absorbance band at 282 nm is present in each sample. As the DMPS:Au ratio decreases in the synthesis, the 282 nm band becomes less dominant while the lower energy absorbance in the visible range intensified. Further increase of the dithiol:Au ratio does not lead to further enhancement of the intensity of 282 nm peak (the spectra of 6× DTC and 6× intermediate completely overlaps with 3× samples thus omitted). Surface plasmon (SP) band at ~520 nm can only be distinguished in the spectrum of 0.5× sample, indicating the Au core sizes of other Au DTCs are less than 2 nm.[16,44,45] In comparison, the synthesis with 1× monothiol (0.5× dithiol) always produces larger Au MPCs that display a more obvious SP band. The gain of entropy by employing dithiol over monothiol in the synthesis obviously altered the cluster formation. Based on previous studies of monothiol MPCs, in which lower thiol:Au ratio synthesis produces larger particles that display higher absorbance at lower energies (visible range), the absorbance features suggest that the Au core size of DTCs decrease from 0.5× to 3×. However, the spectra of 6× (not shown) and 3× DTCs overlap, indicating that further increase of dithiol ratio (more than 3×) does not affect the size distribution of Au-DTCs. The finding suggests that the synthesis with 3× dithiol has already produced the smallest stable clusters under the experimental conditions, and is supported by the results presented next.

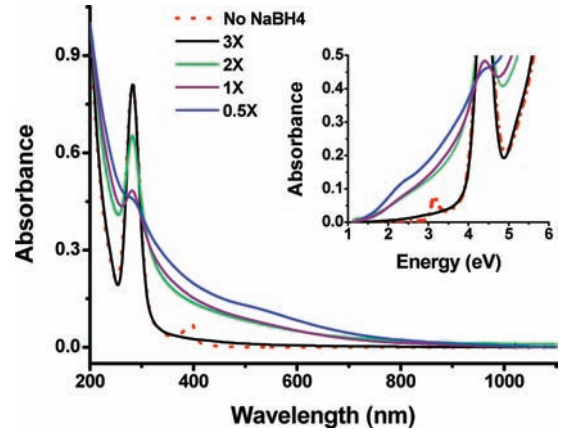

Figure 2. UV−visible absorbance spectra of DMPS Au DTCs. Solid lines from bottom to top at 400 nm represent the spectrum from 3×, 2×, 1×, and 0.5× samples. Spectrum of dashed line is the intermediate of 3× sample before the addition of $NaBH_4$. Inserted are the same data plotted in energy instead of wavelength. The comparison of all intermediates can be found in Supporting Information, Figure SI-1.

The absorbance spectra of all intermediates (3×−0.5×), generally believed to be polymeric complexes and confirmed by mass spectrum discussed next, are included in Supporting Information, Figure SI-1. At dithiol:Au ratio larger than 1×, the intermediates feature similar absorbance bands at ~282 and 395 nm, similar to those observed by Tsukuda and co-workers.[35] This could result from the unique one or a few species present in the intermediates, which have been theoretically predicted in the case of monothiol−Au interactions.[46] The energy states that correspond to the lower-energy absorption band disappear upon the reduction by $NaBH_4$, which indicates that the energy state of the corresponding species was filled during the reduction or that the species in the mixture changed its chemical composition. This is confirmed by the change of mass spectrum and will be further probed by the ongoing separation attempts.

In the inserted plot in Figure 2 the optical band gap from the 3× sample after the addition of $NaBH_4$ can be identified as ~4.0 eV, while other samples are identified at about 1.5 eV. The band gap of each intermediate is larger than 2.5 eV. The characteristic 282 nm absorption band, or 4.0 eV gap, is in excellent agreement with the predicted Au_4 cluster/intermediate that has been identified as a common stable species in several monothiol MPCs.[25,46]

(39) Templeton, A. C.; Chen, S.; Gross, S. M.; Murray, R. W. *Langmuir* **1999**, *15*, 66–76.
(40) Cliffel, D. E.; Zamborini, F. P.; Gross, S. M.; Murray, R. W. *Langmuir* **2000**, *16*, 9699–9702.
(41) Hostetler, M. J.; Wingate, J. E.; Zhong, C. J.; Harris, J. E.; Vachet, R. W.; Clark, M. R.; Londono, J. D.; Green, S. J.; Stokes, J. J.; Wignall, G. D.; Glish, G. L.; Porter, M. D.; Evans, N. D.; Murray, R. W. *Langmuir* **1998**, *14*, 17–30.
(42) Schaaff, T. G.; Whetten, R. L. *J. Phys. Chem. B* **2000**, *104*, 2630–2641.
(43) Peterson, R. R.; Cliffel, D. E. *Anal. Chem.* **2005**, *77*, 4348–4353.
(44) Chen, S.; Ingram, R. S.; Hostetler, M. J.; Pietron, J. J.; Murray, R. W.; Schaaff, T. G.; Khoury, J. T.; Alvarez, M. M.; Whetten, R. L. *Science* **1998**, *280*, 2098–2101.
(45) Negishi, Y.; Takasugi, Y.; Sato, S.; Yao, H.; Kimura, K.; Tsukuda, T. *J. Am. Chem. Soc.* **2004**, *126*, 6518–6519.
(46) Gronbeck, H.; Walter, M.; Hakkinen, H. *J. Am. Chem. Soc.* **2006**, *128*, 10268–10275.

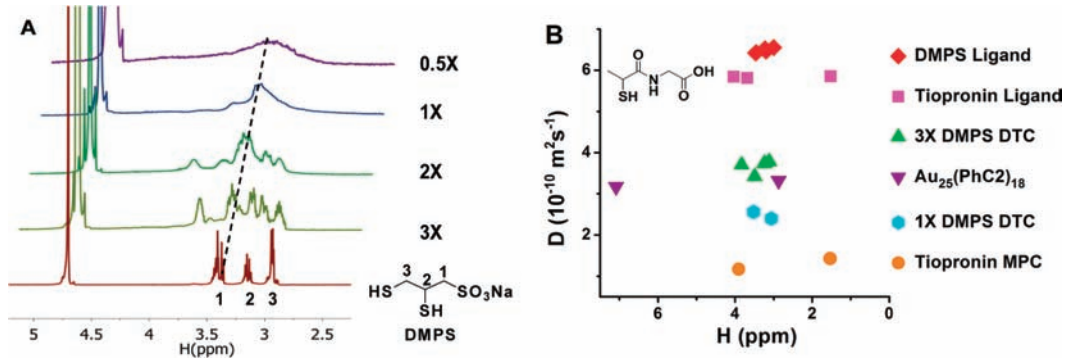

Figure 3. (A) NMR spectra of DMPS ligand and Au-DTCs. The sharp peak at 4.70 ppm is from residual protons in D_2O. Dashed line illustrates the same chemical shift in each spectrum. The spectrum of the 6× sample is the same as the 3× sample (not shown). (B) Comparison of diffusion coefficient calculated from diffusion NMR studies. For convenience, the molecular structure of the tiopronin ligand is inserted.

Hydrodynamic Size Distribution of DMPS DTCs by NMR Studies. Upon Au−S bond formation, the NMR signals of ligand protons will shift as the chemical environment changes. Line broadening is observed due to the slower diffusion, a consequence of the formation of bulky MPCs.[47−49] The effect has been used to confirm the removal of nonbonded thiols and other organic molecules in purification.[41,47,48] One-dimensional proton NMR spectra of free DMPS ligand and purified DTCs (0.5×, 1×, 2×, and 3×) are presented in Figure 3A. Each spectrum is aligned as illustrated by the dashed line; the sharp peak at 4.70 ppm originating from the residual HOD in D_2O solvent. Compared to the free DMPS ligand, significant shifts of ligand C2 and C3 proton signals (at ∼3.14 and 2.92 ppm) and line broadening effect are observed from DMPS DTCs, indicating complex formation. The thiol proton (−S<u>H</u>) signals are missing due to their fast exchange with D_2O. Significant line broadening effect can be observed in the spectrum of the 0.5× DTCs, from which a small SP band in the absorbance spectrum can be found. As the ratio of DMPS:Au increases, there is less line broadening, indicating the DTC size becomes smaller. The trend agrees well with the absorbance features. For 3× and 6× DTCs (overlapping with 3×, not shown), five magnetically different proton peaks are identified and further discussed in the 2D NMR results.

In contrast to imaging on solid surface or invasive MS studies, the hydrodynamic size of the Au DTCs, revealing the natural states of the DTCs in solution, can be estimated on the basis of the Stokes−Einstein equation.[50]

$$D = \frac{kT}{6\pi\eta r}$$

In this equation, k is Boltzmann constant at 1.38×10^{-23} $m^2 \cdot kg \cdot s^{-2} \cdot K^{-1}$; T is temperature; η is viscosity of the solvent, and r is the radius of the analyte. At 25 °C the viscosity of D_2O is 1.10×10^{-3} $Pa \cdot s^{-1}$.[48] From any known or measured diffusion coefficient (D), the hydrodynamic radius (r) can be determined accordingly. Therefore, the size differences of DTCs reflected in the broadening of proton peaks can now be quantified indirectly by DOSY technique, as larger sized DTCs would display slower diffusion. The underlying assumption is that DTCs are in spherical shapes. From a DOSY spectrum, representative proton peaks from a chemical are selected to extract the diffusion coefficient (D) of corresponding species, by Stejskal−Tanner exponential fitting of peak intensity versus the z-axis gradient strength with the error ±5%.[51] Definite diffusion coefficients can be obtained by this method for species with well-resolved NMR signals and significant differences in diffusion coefficient. If the components in the sample mixture have overlapped NMR signals, similar diffusion coefficients, or high molecular weight dispersity such as polymers, Stejskal−Tanner exponential fitting outputs an estimated average diffusion coefficient.[52,53] The results obtained by Stejskal−Tanner exponential fitting are presented in Figure 3, panel B. Tiopronin MPC (with ligand-to-gold mole ratio being 3 in the synthesis, average composition of $Au_{201}Tio_{85}$), $Au_{25}PhC2_{18}$ MPC, and tiopronin, and DMPS ligands, with known average size or molecular weight, were used as references to characterize the newly synthesized DTCs. DOSY experiment of $Au_{25}PhC2_{18}$ MPCs was performed in $CDCl_3$. The presented data have been corrected for solvent viscosity with the assumption that no significant hydrodynamic size differences exist for the MPCs between solvent D_2O and $CDCl_3$. The two ligands (∼200D MW) display faster diffusion compared to that of the Au clusters. The diffusion coefficient decreases in the sequence of 3× DMPS DTCs, the corrected Au_{25} sample, 1× DMPS DTC, and tiopronin MPC. As the average core size of tiopronin MPC was reported to be ∼1.8 nm (without ligand) and has no SP band in the absorbance spectrum, the 1× sample is estimated to be smaller than Au_{201} (tiopronin MPC) but larger than Au_{25}, which is also supported by the featureless absorbance spectrum (the 282 nm peak will be addressed separately). It is interesting to find that the 3× sample is smaller than Au_{25}, consistent with the less obvious peak broadening observed in 1D proton NMR spectrum. Known to be polydispersed, only 1× DTC was tested to demonstrate the size differences. Isolated monodisperse samples would provide more definitive results.

Table 1. Hydrodynamic Sizes of Monothiol and Dithiol Clusters

	3× DMPS DTC	1× DMPS DTC	3× tiopronin MPCs	3× tiopronin MPCs[48]
D (10^{-10} $m^2 \cdot s^{-1}$)	3.92	2.51	1.43	1.4−1.7
radius (nm)	0.51	0.79	1.39	1.4−1.2

The hydrodynamic radius of the DTCs are calculated using Stokes−Einstein equation and are reported in Table 1. The results of home-synthesized tiopronin MPCs and those in the

(47) Parker, J. F.; Choi, J.-P.; Wang, W.; Murray, R. W. *J. Phys. Chem. C* **2008**, *112*, 13976–13981.
(48) Kohlmann, O.; Steinmetz, W. E.; Mao, X. A.; Wuelfing, W. P.; Templeton, A. C.; Murray, R. W.; Johnson, C. S. *J. Phys. Chem. B* **2001**, *105*, 8801–8809.
(49) Donkers, R. L.; Lee, D.; Murray, R. W. *Langmuir* **2004**, *20*, 1945–1952.
(50) Wuelfing, W. P.; Templeton, A. C.; Hicks, J. F.; Murray, R. W. *Anal. Chem.* **1999**, *71*, 4069–4074.

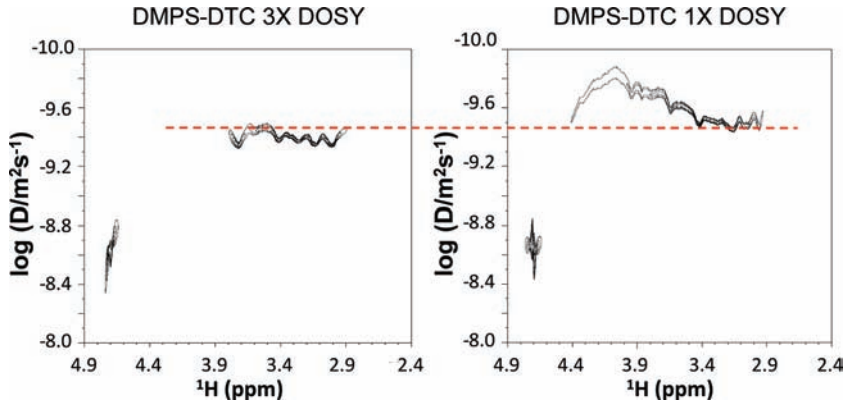

Figure 4. ^{1}H DOSY spectra of 3× and 1× DMPS Au DTCs. The signal at 4.7 ppm is from residual water in D_2O. The dashed line is added to aid the comparison.

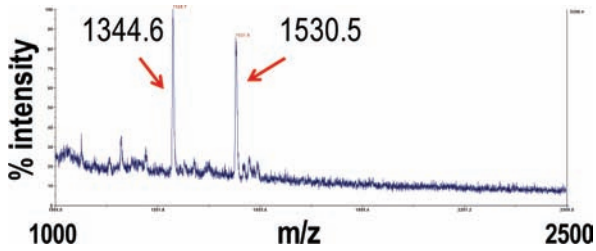

Figure 5. MALDI MS results of the 3× DMPS Au-DTCs. The results were collected under linear negative mode using widely used protein matrix CHCA (α-cyano-4-hydroxycinnamic acid). No signal was detected in higher *m*/*z* region. The two labeled peaks at 1344.6 and 1530.5 *m*/*z* were attributed to Au_4L_3 and Au_4L_4, respectively.

literature are included, through which excellent agreement can be found as a reference.

Complete DOSY spectra of 3× and 1× DMPS DTC samples are presented in Figure 4. The logarithm of diffusion coefficient ($m^2 \cdot s^{-1}$) is plotted against proton chemical shifts (ppm). A very narrow distribution of the log *D*, ranging from −9.32 to −9.49 for all ligand proton signals, is detected from the 3× sample. The signal can be assigned to individual species of same or similar sizes, as log *D* has an error range of ± 0.1 due to the mathematic processing. However, the 1× sample has a much wider range of log *D*, from −9.42 to −9.76, suggesting a mixture of polydispersed species. The upfield species has faster diffusion with log *D* from −9.42 to −9.55 while the low-field species moves much slower with log *D* of −9.76. Although the majority of 1× sample moves slower, the log *D* range of upfield species in 1× sample partly overlaps with that of the 3× sample, indicating components of same or comparable hydrodynamic sizes present in both samples. Considering the common 282 nm absorbance band, the results suggest a common species in each sample but with a different abundance.

Composition of 3× DMPS DTCs by MALDI-MS Studies. The Au-DTCs were analyzed by matrix assisted laser desorption ionization (MALDI) MS in an attempt to identify the molecular ion/s.[26,42] The MALDI results of the 3× sample detected in linear negative mode are presented in Figure 5. Mass features below 1000 are not included due to overlapping with the matrix backgrounds. No detectable peak is observed above 2000 *m*/*z*. Two abundant species can be identified. The accurate values of *m*/*z* 1344.6 and *m*/*z* 1530.5 are calibrated with the results under reflectron mode included in Figure SI-2 (Supporting Information), collected using a separately synthesized 3× sample that has different polydispersity (and thus, cannot be directly compared to NMR and other related results discussed in the main text). If the cluster has one ligand with a deprotonated sulfonate group, the composition of Au_4L_3 and Au_4L_4 would have *m*/*z* 1344.7 and *m*/*z* 1530.7, respectively. The well-matched numbers confirm that both thiol groups have been converted into thiolates. It is worth pointing out that the relative abundance of the two peaks varies from sample to sample, as could be observed in Figures 5 and SI-2 (Supporting Information). This suggests that Au_4L_3 exists in the original sample instead of being a fragment of Au_4L_4. The argument is supported by the TGA results presented at the end. It is also interesting to find that stand-alone Au dithiol clusters share the same Au composition with the Au_4 unit, a key component in monothiol MPCs and as inorganic complexes with crystal structure resolved.[54] Known to be polydisperse, other Au DTCs were not thoroughly studied with MS, but multiple peaks have been observed over wide *m*/*z* ranges.

An interesting pattern reflecting polydisperse species has been detected from the 3× intermediate shown in Figure SI-3 (Supporting Information). The species could be generally described as $Au_xL_y(Au-S)_z$. In the specific spectra, those species with reasonable intensity have the composition of *x* ranging from 5 to 25, *y* ranging from 2 to 3, and *z* ranging from 2 to 8. Signals correponding to Au_4 clusters can also be found. Combined with NMR results, the 282 nm absorbance band is assigned to Au_4 clusters, dominant species in the samples synthesized with dithiol:Au ratio larger than 3×. The abundance of Au_4 clusters decreases as the ratio decreases and the total absorbance is determined by clusters of larger sizes.

Size on a Solid Support Imaged by AFM. Size transition of DMPS DTCs are confirmed by AFM. The sample solution was drop-cast onto freshly cleaved mica before imaging under ambient conditions. Images from 1× and 3× DTCs are presented in Figure 6. The tip radius is ∼10 nm, which limits the lateral resolution. From the height profiles shown in the section panel, the size of the particles can be analyzed. Unlike TEM in which ligands are not observed, the ligand monolayer

(51) Barjat, H.; Morris, G. A.; Smart, S.; Swanson, A. G.; Williams, S. C. R. *J. Magn. Reson. B* **1995**, *108*, 170–172.
(52) Thurecht, K. J.; Howdle, S. M.; Davis, A. L.; Hyde, J. R. *Macromolecules* **2007**, *40*, 976–982.
(53) Morris, K. F.; Johnson, C. S. *J. Am. Chem. Soc.* **2002**, *114*, 3139–3141.
(54) (a) Bau, R. *J. Am. Chem. Soc.* **1998**, *120*, 9380–9381. (b) Schneider, J.; Lee, Y.-A.; Perez, J.; Brennessel, W. W.; Flaschenriem, C.; Eisenberg, R. *Inorg. Chem.* **2008**, *47*, 957–968. (c) Abdou, H. E.; Mohamed, A. A.; Fackler, J. P. *Inorg. Chem.* **2007**, *46*, 141–146.

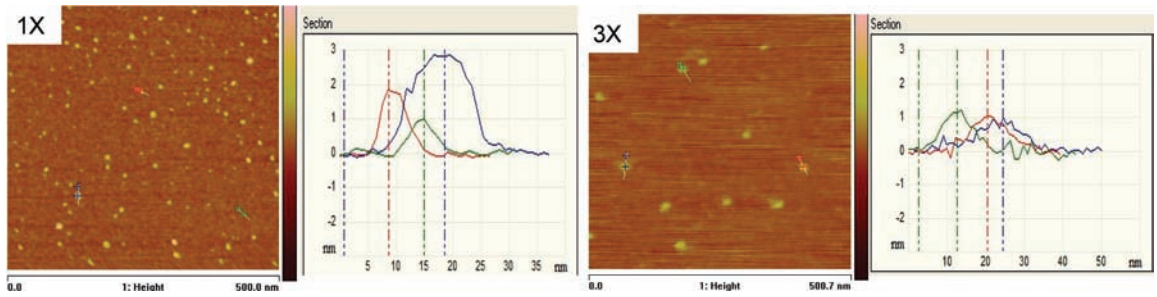

Figure 6. Representative AFM images of 1× and 3× DTCs. The scale of the color bar is 5 nm for 1× sample and 4 nm for 3× sample. The right panel is the section plot presenting the height profiles of three randomly selected particles on mica surface.

is part of the height measured by AFM. Averaged by 80−120 surface particles, the overall size of the 1× sample is found to be 1.5 ± 0.6 nm, while that of the 3× is 1.0 ± 0.3 nm. Much larger size distribution was observed from the 0.5× sample, ranging from ∼2 to 5 nm. The trends agree well with optical and NMR results. The heights of 3× and 1× DTCs find excellent agreements with those calculated by diffusion NMR (twice of the hydrodynamic radius).

Chemical Environments of 3× DMPS DTCs Revealed by NMR 2D ^{13}C−^{1}H HSQC. The experimental design of employing dithiol over monothiol is to tailor the bond structure and thus the property of Au clusters and nanoparticles. Whether dithiol would alter the 'staple' bonding motif depends on whether only one or both thiol groups on one dithiol molecule form Au−S bonds. Such information could be provided by X-ray studies. However, single crystals are difficult to obtain. Consequently, we resort to NMR chemical shift changes to address this issue.

The chemical shifts of the C2 and C3 protons are expected to exhibit significant changes upon Au−S bond formation; therefore, full assignment of individual peaks in 3× Au-DTC NMR spectrum is required. The assignment of proton and carbon resonances was accomplished using COSY, TOCSY and ^{13}C−^{1}H HSQC 2D NMR experiments. In the ^{13}C−^{1}H HSQC spectrum of 3× DTCs presented in Figure 7, each pair of cross peaks (two projections on proton axes symmetric to the 1D peak, and one projection on carbon) represents a unique C−H bond characterized by corresponding ^{1}H and ^{13}C chemical shifts projected on each axis, as indicated in Figure 7.[55] During the preparation of this manuscript, we noticed that a similar approach has recently been attempted to resolve a well-established Au_{25}PhC2 MPC system.[56] In this edited HSQC, the signals from CH (C2, middle peak at ∼49.1 ppm) can be readily differentiated from CH_2 groups (C1 and C3) by the phase differences of the signals and the fact that C2 is only coupled to a single proton. The peak at ∼57.1 ppm is assigned to C1 (attached directly to the sulfonate) according to the chemical shift of the DMPS ligand. The assumption is that its chemical shift of C1 is not changed significantly since it is not the carbon immediately next to the S−Au bond. This assignment is created for the purpose of relative comparison of chemical shift changes of C2 and C3 with respect to C1 before and after bond formation. The high-field signal at ∼43.1 ppm is thus attributed to C3. Compared to free DMPS (C1 57.1 ppm, C2 38.6 ppm, and C3 32.5 ppm), both C2 and C3 signals are shifted by 10.5 and 10.6 ppm, respectively, indicating both C2 and C3 carbon

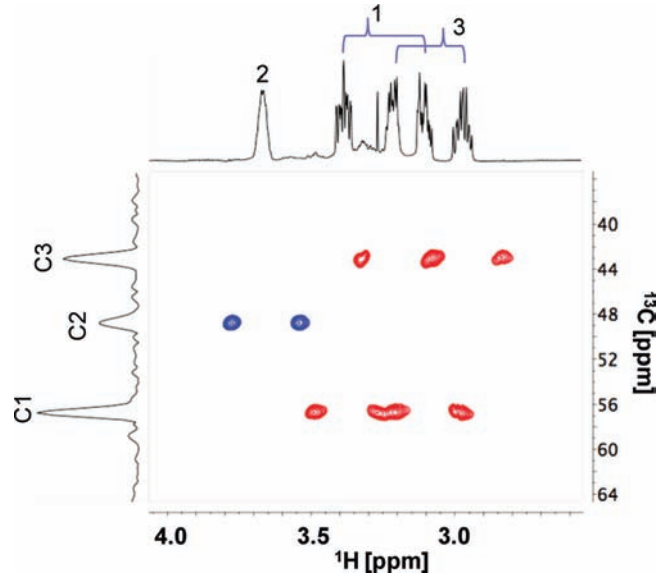

Figure 7. ^{13}C−^{1}H multiplicity edited F2 coupled HSQC spectrum of 3× DMPS Au DTCs. The vertical and horizontal axes represent ^{13}C and ^{1}H chemical shifts. Positive contours (blue) correspond to CH, and negative contours (red) are from CH_2 groups. The cross peaks originating from the same C−H are separated by the $^{1}J_{CH}$ coupling. Assignments are indicated on the 1D projections.

atoms experience similar changes in the chemical environment upon Au−S bond formation. This suggests both −SH sites participate in the formation of Au−S bonds for each DMPS ligand.

These observations are further supported by the proton spectra where significant chemical shift differences are also noted. The C2 proton, shifts from 3.14 ppm in the free ligand to 3.65 ppm, indicating S−Au bond formation. In the free ligand the protons of the methylene group C1 are degenerate as are those of C3. Upon complex formation the C1 methylene group protons (3.38 ppm) become nonequivalent and resonate at 3.42 and 3.10 ppm. Similarly, the two protons of C3 which resonate at 2.92 ppm in the free ligand appear at 3.20 and 2.95 ppm. For both C2 and C3 one proton experiences significant chemical shift changes, signaling significant chemical environment changes due to the formation of S−Au bond. This is further supported by the results of COSY and TOCSY listed in Figures SI-4 and SI-5 (Supporting Information). Additionally, the nonequivalence of the C2 and C3 methylene protons suggests that the ligand is constrained after complex formation. The ligands with limited flexibility are in line with our proposed structure presented at the end. The Au_4L_4 and Au_4L_3 complexes, detected by MALDI-MS, are not differentiated by NMR. In addition to the similarity

(55) Friebolin, H., *Basic One- and Two-Dimensional NMR Spectroscopy* 4th ed.; Wiley-VCH,: 2005; p xxiv, 406 p.
(56) Wu, Z.; Gayathri, C.; Gil, R. R.; Jin, R. *J. Am. Chem. Soc.* **2009**, *131*, 6535–6542.

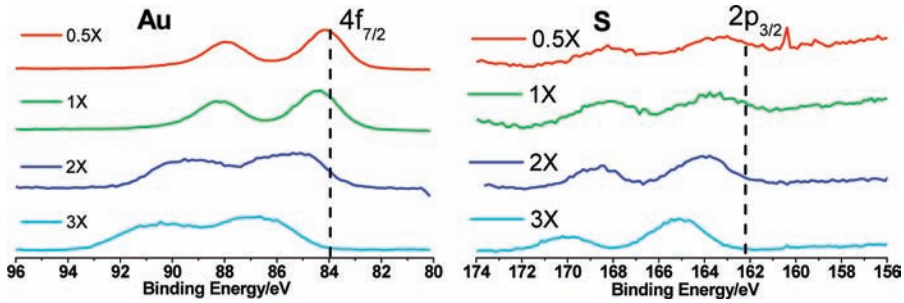

Figure 8. XPS spectra of DMPS DTCs. The binding energy of Au(4f) and S(2p) electrons is presented. Survey scan can be found in Figure SI-6 (Supporting Information).

of the two complexes, making it challenging to resolve, there is a possibility that the Au_4L_3 originates from the fragmentation of Au_4L_4.

X-ray Photoelectron Spectroscopy Studies of Au−S Bonding. The nature of Au dithiol interaction is further probed with XPS. Figure 8 shows the Au(4f) and S(2p) photoemission spectra of DMPS DTCs. The presence of −Cl and −Br were ruled out by the survey scan (SI-6 in Supporting Information). In the case of monothiol MPCs, the binding energy (BE) of Au($4f_{7/2}$) increases as the MPC size decreases, ranging from Au(0) film of ∼83.8 eV up to Au(I) compounds of ∼86.0 eV.[16,41,57] From 0.5× to 2× DMPS DTCs, the BE of Au($4f_{7/2}$) increases, within the range of Au(0) and Au(I). The broadening effect could result from the polydispersity of the sample but has not been ascertained. It is surprising to find that BE of Au($4f_{7/2}$) of 3× sample is larger than that of Au(I) and approaches that of Au(III) ($AuCl_4^-$ at about 86.9 eV).[58] The results suggest that additional charge transfer or bond exists, which is also reported in other metal clusters.[59] The S(2p) spectra display similar trends. The BE of S($2p_{3/2}$) also increases from 0.5× to 3× samples, or from larger to smaller clusters. For reference, the BE of S(2p) from thiol 2D SAM on Au(111) and MPCs ranges from 162.0 to 162.3 eV.[41,60] The peak at higher BE is assigned to the SO_3^- group, which is known to be at ∼168 eV, reflecting oxidized S. For 3× sample, the BE of S($2p_{3/2}$) is even larger than the S element at 164.2 eV. Considering the sample is synthesized under reduction by $NaBH_4$, the stability of this electron deficient sample compared to the Au(I) thiolates is impressive. Though XPS data were collected after the sample has been synthesized and purified over days with the exposure to air (O_2), the absorbance features of samples immediately after reduction remain unchanged over days/weeks in solution under comparable condition. Some samples do decompose over time (months) presumable due to the presence of oxygen and light.

In the reported monothiol Au_4 ring-like structure, each Au directly interacts with two S atoms. Incomplete charge donation between Au and S observed in these small clusters will generate nonintegral charge states of corresponding atoms. As a matter of fact, charge transfer in Au_4 system has been calculated to be +0.4 eV for Au. S atom,[46] on the other hand, interacts with one carbon atom and two Au atoms. The high BE values of

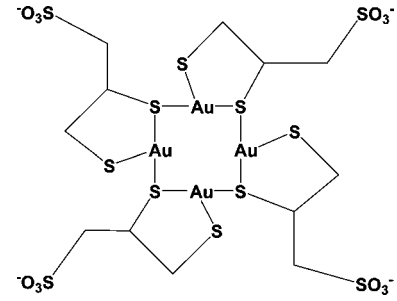

Figure 9. Proposed Au_4L_4 cluster structure.

Au(4f) and S(2p) suggest additional bond or interaction in the 3× DMPS DTCs, which would further change the charge states of Au and S.[59] An extended ring of (Au−S−C−C−S−)$_4$ is basically a Au(I) compound, which is unlikely since both Au and S XPS signals are significantly shifted away from the reported Au(I) thiolate compounds. In conjunction with different chemical environments revealed in proton chemical shifts by NMR, a tentative structure is proposed as shown in Figure 9. A 3D structure (ball−stick) that is relaxed by preliminary molecular mechanics approach can be found in Figure SI-9 (Supporting Information). The Au_4 ring holds off-plane boat-form structure as Au is at ca. positive III states instead of I. An extended Au(I) ring structure, Au_{16} stabilized by phosphine complexes, has been reported.[61] The sulfonate groups are positioned to take trans- configuration, on the opposite sides of the Au plane to minimize the potential charge repulsion. It is not clear how the two thiolate groups on one DMPS ligand replace two individual DMPS ligands to form a stable Au_4L_3 complex. One tentative structure is included in Figure SI-10 (Supporting Information). In the proposed Au_4 structures, Au−Au distances are measured to be ∼4 Å, longer than the Au(I)−Au(I) bond at ∼2.7−2.9 Å previously reported.[21] Based on the proposed structures, the size of the proposed structure is estimated to be ∼1.0 ± 0.1 nm for Au_4L_4 and 0.85 ± 0.1 Au_4L_3 respectively, pending the direction of measurement. The dimension matches reasonably well with experimental results from AFM and diffusion NMR. Further theoretical calculation of energy favored Au_4 structures is underway. The less symmetric Au_4L_3 complex would incur broader features in XPS and other spectra as both Au and S atoms encounter several different chemical environments. It is important to point out that the Au_4 units found in monothiol Au MPCs is located on core surface, which means multiple interactions exist between the inner atoms and the Au_4 units. In the proposed structure, the off-plane

(57) (a) Brust, M.; Walker, M.; Bethell, D.; Schiffrin, D. J.; Whyman, R. *J. Chem. Soc., Chem. Commun.* **1994**, *7*, 801–802. (b) Bain, C. D.; Biebuyck, H. A.; Whitesides, G. M. *Langmuir* **1989**, *5*, 723–727.
(58) Kitagawa, H.; Kojma, N.; Nakajima, T. *J. Chem. Soc., Dalton Trans.* **1991**, *11*, 3121–3125.
(59) Kaden, W. E.; Wu, T.; Kunkel, W. A.; Anderson, S. L. *Science* **2009**, *326*, 826–829.
(60) Shon, Y. S.; Gross, S. M.; Dawson, B.; Porter, M.; Murray, R. W. *Langmuir* **2000**, *16*, 6555–6561.
(61) Yu, S.-Y.; Zhang, Z.-X.; Cheng, E. C.-C.; Li, Y.-Z.; Yam, V. W.-W.; Huang, H.-P.; Zhang, R. *J. Am. Chem. Soc.* **2005**, *127*, 17994–17995.

interactions of Au−S bonds and Au-sulfonate 'ion pairing' stabilize the stand-alone Au_4 clusters.

Further Structural Confirmation and Properties. Au−S bond formation is further confirmed by the disappearance of -SH stretching of the free ligand at 2543 cm^{-1} in the infrared spectrum (SI-7 in Supporting Information). The ligand-to-gold ratio was probed by TGA measurements in Figure SI-8 (Supporting Information). Mass loss corresponding to organic components starting at ~260 °C over the residue is calculated to be 0.85 for 3× sample. Compared to the MS results of Au_4L_3 and Au_4L_4 at almost equivalent abundance, which have L:Au mass ratio of 0.70 and 0.94, respectively, excellent agreement is found from TGA results. The enhanced thermostability of DTCs compared to that of monothiol MPCs affirms the multi-interaction by dithiol ligands with Au and supports the structure proposed.

Near IR luminescence, ranging from ~700 to 1000 nm when excited at higher energy (e.g. 450 nm), observed from Au MPCs with core diameter smaller than 2 nm and mostly with polar ligands,[62−68] is not detected from these DTCs with a full spectrum scan. Not precisely correlated with the MPC energetics, the origin of the luminescence has been postulated to surface localized states.[63,64] It is interesting to notice that one Au atom is positioned away from the core in the thiol bridging surface bond structure. The disappearance of near-IR luminescence from all synthesized DTCs strongly suggests fundamental differences between MPCs and DTCs. Surface bond structures of DTCs of large sizes are currently being studied; they are believed to differ from monothiol MPCs, as different properties in luminescence and place exchange reactions have been observed.[68]

Conclusions

In summary, multidentate ligand DMPS-stabilized Au DTCs have been synthesized at different dithiol:Au ratios. The DTCs have been found to differ significantly in composition, structure, and physical properties with their counterpart monothiol Au MPCs, which reflect the impacts made by the designated dithiol molecular structures. The composition and sizes are analyzed by mass spectrometry and AFM imaging. Believed to be the smallest building units in monothiol MPC systems, stand-alone Au_4 clusters with three or four DMPS ligands have been directly synthesized at high purity. A characteristic 282 nm absorbance band, or a 4.0 eV optical gap in absorbance spectra, has been attributed to the Au_4 DTCs. Diffusion coefficients, reflecting the hydrodynamic size of the DTCs, are reported from diffusion NMR studies. Based on proton and carbon NMR chemical shift information, and with the binding energy of Au(4f) and S(2p) XPS data, thiol bridging surface structure discovered in monothiol MPCs is obviously changed in the Au_4 DTCs, as presented in the proposed structure.

Acknowledgment. We thank Dr. Siming Wang and Yanyi Chen for mass spectrometry measurements. We acknowledge Chun Huang (Department of Chemistry and Biochemistry, Georgia Instuitue of Technology) for his generous help with TGA measurements. We thank Drs. Binghe Wang and Markus W. Germann for the access to the IR and NMR spectrometers. The help from Hui Zhao at Biocore facility at GSU for AFM measurements is acknowledged. The research is supported by the start-up funds and Research Initiation Award at Georgia State University. The discussion of cluster structures and energetics with Dr. Deen Jiang at Oak Ridge National Laboratory is acknowledged.

Supporting Information Available: UV−visible absorbance spectra, mass spectra of pre-DTC intermediates before the reduction by $NaBH_4$, COSY and TOCSY of Au DTCs, XPS survey scan, infrared spectra, thermogravimetric analysis data, the proposed structure of Au_4L_3, and three-dimensional structures of Au_4L_4 and Au_4L_3 by molecular mechanics. This material is available free of charge via the Internet at http://pubs.acs.org.

JA9076149

(62) Link, S.; Beeby, A.; FitzGerald, S.; El-Sayed, M. A.; Schaaff, T. G.; Whetten, R. L. *J. Phys. Chem. B* **2002**, *106*, 3410–3415.
(63) Cheng, P. P. H.; Silvester, D.; Wang, G.; Kalyuzhny, G.; Douglas, A.; Murray, R. W. *J. Phys. Chem. B* **2006**, *110*, 4637–4644.
(64) Wang, G.; Huang, T.; Murray, R. W.; Menard, L.; Nuzzo, R. G. *J. Am. Chem. Soc.* **2005**, *127*, 812–813.
(65) Huang, T.; Murray, R. W. *J. Phys. Chem. B* **2001**, *105*, 12498–12502.
(66) Negishi, Y.; Tsukuda, T. *Chem. Phys. Lett.* **2004**, *383*, 161–165.
(67) Shibu, E. S.; Muhammed, M. A. H.; Tsukuda, T.; Pradeep, T. *J. Phys. Chem. C* **2008**, *112*, 12168–12176.
(68) Tang, Z.; Wang, G. Manuscript in preparation.